



ELSEVIER

Available online at www.sciencedirect.com

SCIENCE @ DIRECT®

C. R. Mecanique 333 (2005) 713–718



MECANIQUE

<http://france.elsevier.com/direct/CRAS2B/>

Computational AeroAcoustics: from acoustic sources modeling to farfield radiated noise prediction

A stable and efficient hybrid method for aeroacoustic sound generation and propagation

Jan Nordström^{a,b,*}, Jing Gong^b

^a *The Department of Computational Physics, Division of Systems Technology, the Swedish Defence Research Agency, 164 90 Stockholm, Sweden*

^b *The Department of Information Technology, Scientific Computing, Uppsala University, 751 05 Uppsala, Sweden*

Available online 9 September 2005

Abstract

We discuss how to combine the node based unstructured finite volume method widely used to handle complex geometries and nonlinear phenomena with very efficient high order finite difference methods suitable for wave propagation dominated problems. This fully coupled numerical procedure reflects the coupled character of the sound generation and propagation problem. The coupling procedure is based on energy estimates and stability can be guaranteed. Numerical experiments using finite difference methods that shed light on the theoretical results are performed. **To cite this article: J. Nordström, J. Gong, C. R. Mecanique 333 (2005).**

© 2005 Académie des sciences. Published by Elsevier SAS. All rights reserved.

Résumé

Une méthode hybride, stable et efficace pour la génération et la propagation acoustique. Nous discutons de la façon de combiner une méthode de volumes finis en maillage non structuré, largement utilisé pour les géométries complexes et les phénomènes non linéaires, avec une méthode très performante de différences finies d'ordre élevé adapté pour les problèmes dominés par la propagation acoustique. Cette procédure numérique fortement couplée rend compte du caractère couplé des phénomènes de génération et de propagation acoustique. La procédure de couplage est basée sur des estimations de l'énergie et la stabilité peut être alors garantie. Les expériences numériques utilisant les méthodes de différences finies, en regard des résultats théoriques, sont réalisées. **Pour citer cet article : J. Nordström, J. Gong, C. R. Mecanique 333 (2005).**

© 2005 Académie des sciences. Published by Elsevier SAS. All rights reserved.

Keywords: Acoustics; Aeroacoustics; Sound generation; Sound propagation; Hybrid method; Stability; Accuracy

Mots-clés: Acoustique; Aéroacoustique; Génération du son; Propagation du son; Méthode hybride; Stabilité; Précision

* Corresponding author.

E-mail addresses: Jan.Nordstrom@foi.se (J. Nordström), Jing.Gong@it.uu.se (J. Gong).

1. Introduction

The computation of aeroacoustic sound can in many applications be divided into two parts: (i) The computation of the source in the near field by solving the nonlinear fluid flow equations; (ii) the calculation of sound propagation to the far field by solving linear equations. Sometimes the coupled character of the problem, i.e. the fact that the sound source influence the sound propagation and that the sound propagation influence the nature of the source, is important. In those cases, the coupling must be kept in the computational procedure for a correct result.

In computational fluid dynamics, node based unstructured finite volume methods are widely used to handle complex geometries and nonlinear phenomena. It is also clear that high order finite difference methods are very efficient for wave propagation dominated problems such as computational aeroacoustics and computational electromagnetics.

In this paper we will discuss how to combine the finite volume method described and analyzed in [1] with the finite difference methods considered in [2–4]. In real life calculations, the finite volume method will mainly be used close to the sound source where complex geometries and nonlinear phenomena are important while the highly efficient finite difference method are ideally suited for the pure sound propagation part in the far field.

Both these methods employ so-called summation by parts (SBP) operators and impose the boundary conditions weakly. This specific character of the methods enables us to couple these different methods together in a stable way. Moreover, it can be shown that a strictly stable procedure which is important for long time calculations on realistic meshes can be obtained, see [1–4].

In a forthcoming paper we will show in detail how to combine the finite volume method with the finite difference method in a truly stable way. Here we will indicate how to obtain those results and exemplify the whole procedure by using finite difference methods.

2. Analysis

The continuous problem we are interested in is of the general form:

$$u_t + Au_x + Bu_y = 0, \quad (x, y) \in \Omega \subset \mathbb{R}^2 \quad (1)$$

with suitable boundary and initial conditions. In (1), u is the vector of unknowns and A and B are constant, symmetric, square matrices with m rows and columns. For aeroacoustic applications we can consider (1) to be the symmetrized Euler equations. The energy method applied to (1) gives

$$\frac{d}{dt} \|u\|_{\Omega}^2 = - \oint_{\partial\Omega} u^T (A\hat{x} + B\hat{y})u \cdot \hat{n} \, ds \quad (2)$$

with the use of Greens formula and the symmetry of A and B . In (2), $\|u\|^2 = \int u^2 \, dx \, dy$, \hat{n} is the outward pointing unit normal to $\partial\Omega$, \hat{x} and \hat{y} are the unit vectors in the x - and y -directions and ds is the infinitesimal arc length element counted counter clockwise around Ω .

The number of boundary conditions at any point on the boundary is equal to the number of negative eigenvalues of $(A\hat{x} + B\hat{y}) \cdot \hat{n}$. When referring to the problem (1), it is assumed that the boundary conditions are such that this is true.

2.1. The two different numerical approximation methods

Let u denote a grid function and u_x its exact derivative projected onto the same grid. We call $D = P^{-1}Q$ an $(n + 1)$ th order accurate approximation of the first derivative operator if

$$Du = u_x + [\mathcal{O}(h^n), \dots, \mathcal{O}(h^{2m}), \dots, \mathcal{O}(h^n)]^T \quad (3)$$

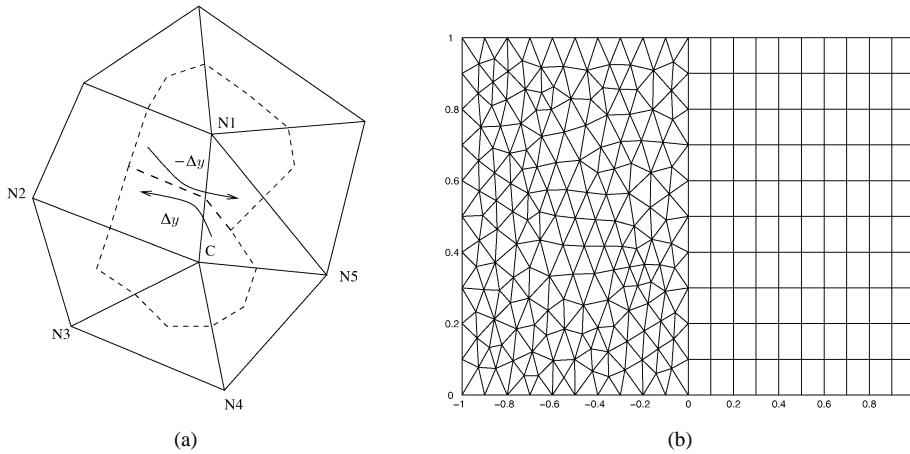


Fig. 1. (a) The unstructured grid (solid line) and the dual grid (dashed line); (b) a hybrid grid with an interface.
 Fig. 1. (a) Maillage non structuré (trait plein) et maillage dual (tireté); (b) maillage hybride avec une interface.

where $2m > n$. The operator $D = P^{-1}Q$ is an SBP operator if (i) the matrix P is symmetric and positive definite and defines a scalar product $(u, v)_P = u^T P v$ and a norm $\|u\|_P^2 = (u, u)_P$ and (ii) the matrix Q is nearly skew-symmetric and $Q + Q^T = B$, where B is diagonal such that $B = \text{diag}[-1, 0, \dots, 0, 1]$. These properties yield,

$$(u, Du) = u^T P D u = u^T Q u = u_N^2 - u_0^2 - (Du, u)$$

which completely mimics integration by parts. $2m$ th order accuracy in (3) require $n = 2m - 1$ and a P which have blocks at the upper left and lower right corners. With a purely diagonal P , we can obtain an SBP operator if $n = m$ which leads to $(m + 1)$ th order accuracy.

We can couple one type of finite difference method to another but also to a node based finite volume methods if we use diagonal norms in the finite difference method. We consider finite volume approximations of the difference operators such that

$$D_x = P^{-1}Q_x, \quad D_y = P^{-1}Q_y, \quad Q_x + Q_x^T = Y, \quad Q_y + Q_y^T = X \tag{4}$$

where P is a diagonal matrix with the control volumes from the dual grid, see Fig. 1(a), on the diagonal. The non-zero elements in Y, X are $\Delta y_i, -\Delta x_i$ respectively and correspond to the boundary points. Eq. (4) shows that also the finite volume scheme is on SBP form since

$$(u, D_x u) = u^T P D_x u = u^T Q_x u = u^T Y u - (D_x u, u)$$

The unstructured finite volume method is at most second order accurate.

Both the finite difference and finite volume scheme described above require a particular boundary treatment in order to obtain stability. There are various techniques but we will use the so-called SAT method developed in [5]. The SAT technique is a penalty procedure that can be used to specify outer boundary conditions as well as treating block interfaces, see Fig. 1(b). For details we refer the reader to [1–5].

2.2. Stable interface treatment

We will discretise (1) on $\Omega: -1 \leq x \leq 1, 0 \leq y \leq 1$ using 2 blocks with an interface at $x = 0$. We consider finite difference methods in both blocks and discretize the domains with n and l points and in the x -direction and k points in the y -direction and denote the $nkm \times 1, lkm \times 1$ vectors u and v , respectively. Note that the grid points at the interface match. The difference operators in the x - and y -direction might be different in the left and right domain and are denoted D_x^L, D_x^R, D_y^L and D_y^R . Further we introduce the following simplifications, $\tilde{I}_L = I_n \otimes I_k \otimes I_m$,

$\tilde{I}_R = I_l \otimes I_k \otimes I_m$, $\tilde{\Sigma}_L = I_n \otimes I_k \otimes \Sigma_L$ and $\tilde{\Sigma}_R = I_l \otimes I_k \otimes \Sigma_R$. The notation \otimes stands for the Kronecker product. By using these notations, the semi-discrete system becomes,

$$\tilde{I}_L u_t + (D_x^L \otimes I_k \otimes A)u + (I_n \otimes D_y^L \otimes B)u = ((P_x^L)^{-1} \otimes I_k \otimes I_m) \tilde{\Sigma}_L (e_N \otimes (u_N - v_0)) + SAT_L \quad (5)$$

$$\tilde{I}_R v_t + (D_x^R \otimes I_k \otimes A)v + (I_l \otimes D_y^R \otimes B)v = ((P_x^R)^{-1} \otimes I_k \otimes I_m) \tilde{\Sigma}_R (e_0 \otimes (v_0 - u_N)) + SAT_R \quad (6)$$

where the right-hand sides are the penalty terms. Σ_R and Σ_L are $m \times m$ matrices that are determined by stability. Note that we have a penalty on $u_N - v_0$ which is the difference between the solution along the interface. The term SAT_L and SAT_R denotes the penalty terms at the outer boundaries. These are scaled to precisely cancel the boundary terms. $e_0 = (1, 0, \dots, 0)^T$ and $e_N = (0, \dots, 0, 1)^T$ are $l \times 1$ and $n \times 1$ vectors, respectively.

In [6], it was shown that the scheme above is stable and conservative if $P_y^L = P_y^R$ and

$$\lambda_L^i < \frac{\lambda^i}{2}, \quad \lambda_R^i = \lambda_L^i - \lambda^i \quad (7)$$

where $i = 1, \dots, m$. In (7), λ^i is the i th eigenvalue of the symmetric matrix $A = X \Lambda X^T$ where X contains the eigenvectors of A . We have also assumed that $\Sigma_L = X \Lambda_L X^T$ and $\Sigma_R = X \Lambda_R X^T$. The first condition in (7) is the stability condition and the second condition is the conservation condition, see for example [2].

It has now been indicated how to couple two different blocks together in a stable way using finite difference methods of SBP type. Note that the computational blocks have to share the points constituting the internal boundaries at each block interface and that the norm along the interface has to be the same at both sides, i.e. we need $P_y^L = P_y^R$. In a forthcoming paper we will show in detail how to couple the building blocks (the finite volume method and the finite difference method) of the final hybrid method, see Fig. 1(b), in a stable way. The stability proof proceeds essentially along the lines described above.

3. Numerical experiments

Numerical experiments that support the basic idea in this paper, namely that it is worthwhile to couple a robust low order method with an efficient high order method in a stable way will be shown. Examples that highlight the stability issues will also be given. We will only consider the finite difference case. Consider the scalar advection problem,

$$u_t + au_x + bu_y = 0, \quad (x, y) \in \Omega \quad (8)$$

with $a, b > 0$ and initial data and boundary data at $x = -1, y = 0$ such that the exact solution is given by $u = \sin(2\pi(x + y - (a + b)t))$. In Fig. 2, the result of a second order and sixth order accurate calculation at $T = 1$ on one domain is shown. A uniform mesh with 81×41 grid points were used. Note the significant difference in error levels.

We move on to calculations on two domains with an interface at $x = 0$. In the calculations shown in Fig. 3, we have used 41×41 grid point in both the left and right domain. In the calculation in Fig. 4(a) we have used 41×41 in the left domain and only 11×41 in the right one. Note that the L_2 -error are of the same size for all calculations. The major part of the error in Fig. 4(a) is created in the left domain (with the dense mesh and low accuracy) and advected into the right domain (with the coarse mesh and high accuracy). This effect can be seen in Fig. 3(b) also.

Finally we will illustrate the importance of stability at the interface. If we apply condition (7) to our model problem (8) we find that it is stable for $\lambda_L < a/2$, $\lambda_R = \lambda_L - a$. In the calculation shown in Fig. 4(b) we have used $\lambda_L = a$. The calculation were done on a mesh with 41×41 grid point in both the left and right domain. The calculation shown in Fig. 4(b) explodes shortly after $T = 0.25$. Note the huge error along the interface. A corresponding calculation using $\lambda_L = 0$ is stable and has $\text{Log}(L_2\text{-error}) = -6.20$ at $T = 1$ which corresponds to the error level in Fig. 2(b).

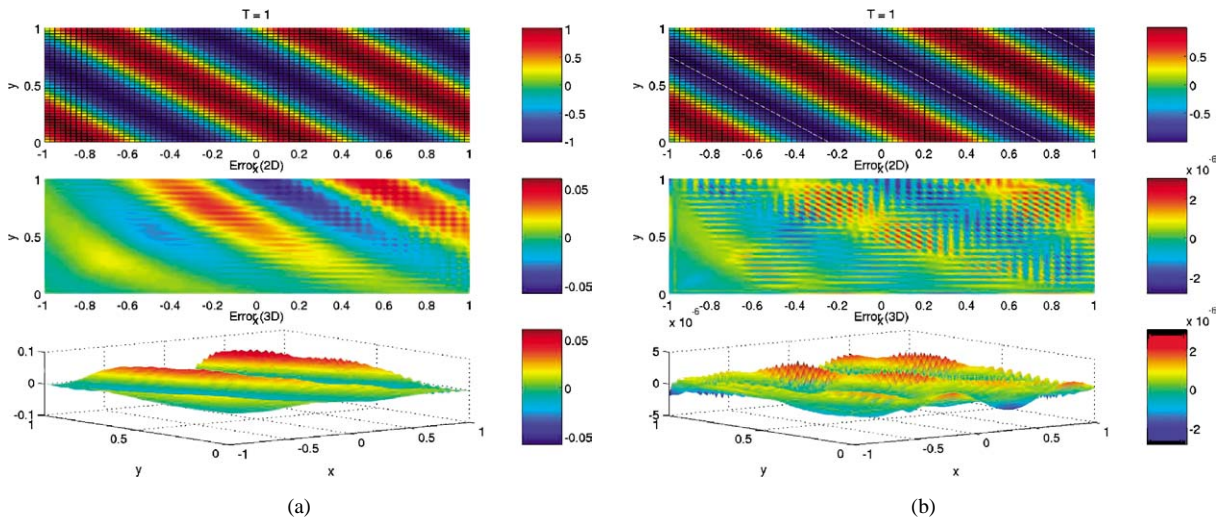


Fig. 2. One domain, (a) second order results, $\text{Log}(L_2\text{-error}) = -1.84$; (b) sixth order results, $\text{Log}(L_2\text{-error}) = -6.21$.

Fig. 2. Un domaine, (a) résultats avec le second ordre, $\text{Log}(L_2\text{-erreur}) = -1,84$; (b) résultats avec le sixième ordre, $\text{Log}(L_2\text{-erreur}) = -6,21$.

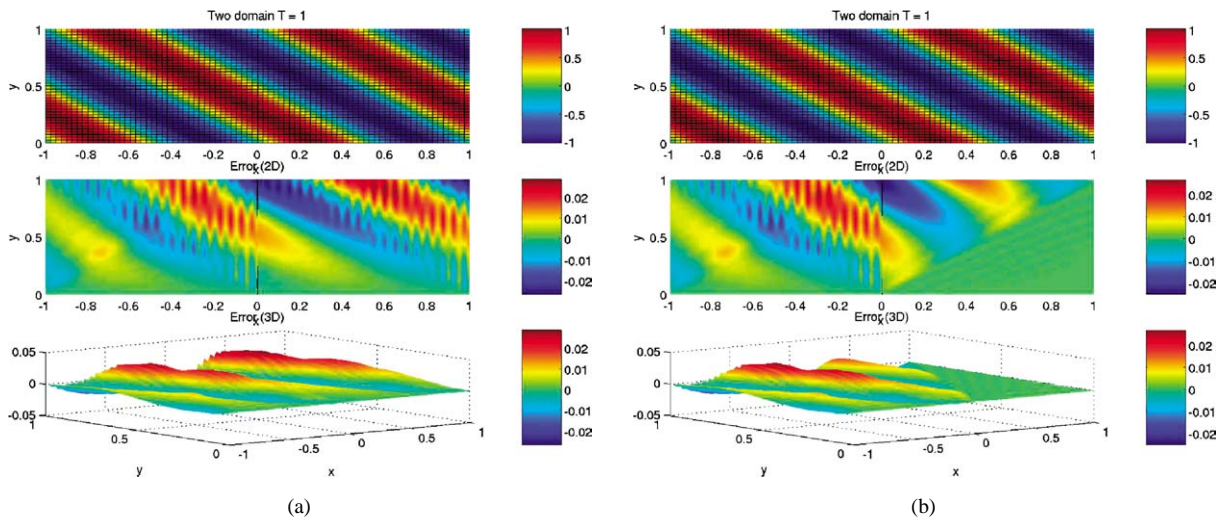


Fig. 3. Both domains are sixth order in y , (a) left and right domain is second order in x , $\text{Log}(L_2\text{-error}) = -2.13$, (b) left is second order in x , right domain is sixth order in x , $\text{Log}(L_2\text{-error}) = -2.24$.

Fig. 3. Les deux domaines avec le sixième ordre en y , (a) les domaines de gauche et de droite avec le second ordre en x , $\text{Log}(L_2\text{-erreur}) = -2,13$, (b) le domaine de gauche avec le second ordre en x , le domaine de droite avec le sixième ordre, $\text{Log}(L_2\text{-erreur}) = -2,24$.

4. Conclusions

It has been discussed how to combine the node based unstructured finite volume method widely used to handle complex geometries and nonlinear phenomena with very efficient high order finite difference methods suitable for wave propagation dominated problems.

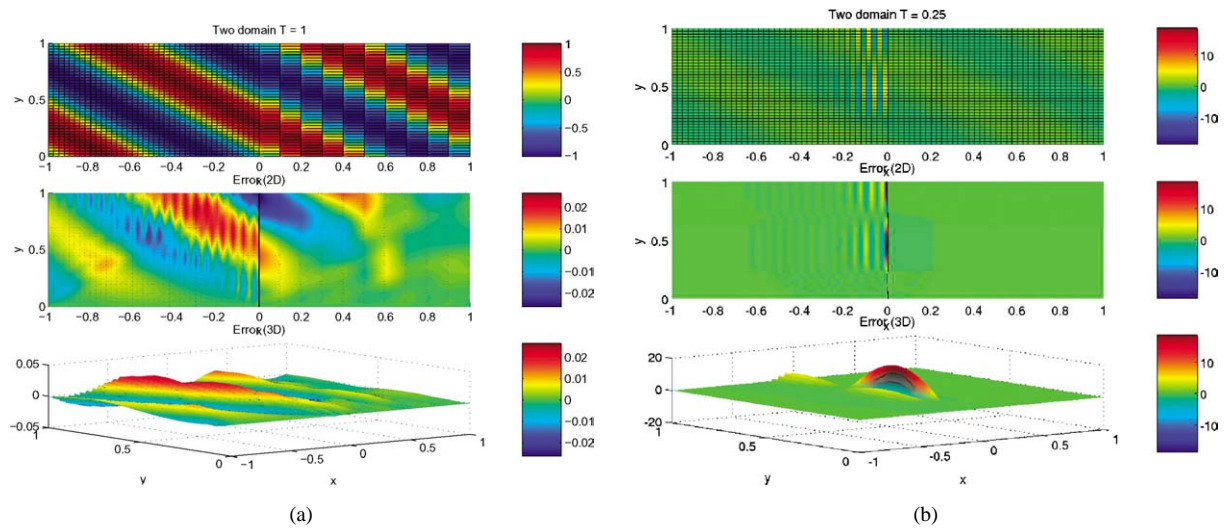


Fig. 4. (a) Left domain is second order in x , right domain is sixth order in x , both domains are sixth order in y , $\text{Log}(L_2\text{-error}) = -2.22$; (b) sixth order accurate operators with an unstable interface treatment.

Fig. 4. (a) Le domaine de gauche avec le second ordre en x , le domaine de droite avec le sixième ordre, les deux domaines avec le sixième ordre en y , $\text{Log}(L_2\text{-erreur}) = -2,22$; (b) opérateurs du sixième ordre avec un traitement de l'interface instable.

The coupling procedure is based on energy estimates and stability can be guaranteed. Numerical experiments using finite difference methods that exemplify the theoretical discussions have been presented.

The calculations show that increased efficiency and accuracy can be obtained using hybrid methods. It has also been shown that the key to accurate results are stable interface treatments.

References

- [1] J. Nordström, K. Forsberg, C. Adamsson, P. Eliasson, Finite volume methods, unstructured meshes and strict stability, *Appl. Numer. Math.* 48 (2003) 453–473.
- [2] M.H. Carpenter, J. Nordström, D. Gottlieb, A stable and conservative interface treatment of arbitrary spatial accuracy, *J. Comput. Phys.* 148 (1999) 341–365.
- [3] J. Nordström, M.H. Carpenter, Boundary and interface conditions for high order finite difference methods applied to the Euler and Navier–Stokes equations, *J. Comput. Phys.* 148 (1999) 621–645.
- [4] J. Nordström, M.H. Carpenter, High-order finite difference methods, multidimensional linear problems, and curvilinear coordinates, *J. Comput. Phys.* 173 (2001) 149–174.
- [5] M.H. Carpenter, D. Gottlieb, S. Abarbanel, Time-stable boundary conditions for finite-difference schemes solving hyperbolic systems: methodology and applications to high-order compact schemes, *J. Comput. Phys.* 111 (1994) 220–236.
- [6] K. Mattsson, M. Svård, M.H. Carpenter, J. Nordström, J. Accuracy requirements for transient aerodynamics, in: *The 16th AIAA CFD Conference*, AIAA 2003-3689, Orlando, FL, 2003.